

AD A137244

12  
ESL-TR-82-50

# EVALUATION OF NASA STRUCTURAL ANALYSIS (NASTRAN) TO PREDICT THE DYNAMIC RESPONSE OF REINFORCED CONCRETE

WILLIAM W. PAYME, JR.

AIR FORCE ENGINEERING AND SERVICES CENTER  
ENGINEERING AND SERVICES LABORATORY  
TYNDALL AIR FORCE BASE, FLORIDA 32413

DECEMBER 1983

FINAL REPORT  
27 MAY 1981 - 5 AUGUST 1981

DTIC  
REFLECTED  
JAN 26 1984

A

APPROVED FOR PUBLIC RELEASE; DISTRIBUTION UNLIMITED

DTIC FILE COPY



ENGINEERING AND SERVICES LABORATORY  
AIR FORCE ENGINEERING AND SERVICES CENTER  
TYNDALL AIR FORCE BASE, FLORIDA 32403

84 01 26 058

NOTICE

PLEASE DO NOT REQUEST COPIES OF THIS REPORT FROM  
HQ AFESC/RD (ENGINEERING AND SERVICES LABORATORY).  
ADDITIONAL COPIES MAY BE PURCHASED FROM:

NATIONAL TECHNICAL INFORMATION SERVICE  
5285 PORT ROYAL ROAD  
SPRINGFIELD, VIRGINIA 22161

FEDERAL GOVERNMENT AGENCIES AND THEIR CONTRACTORS  
REGISTERED WITH DEFENSE TECHNICAL INFORMATION CENTER  
SHOULD DIRECT REQUESTS FOR COPIES OF THIS REPORT TO:

DEFENSE TECHNICAL INFORMATION CENTER  
CAMERON STATION  
ALEXANDRIA, VIRGINIA 22314

UNCLASSIFIED

SECURITY CLASSIFICATION OF THIS PAGE (When Data Entered)

REPORT DOCUMENTATION PAGE		READ INSTRUCTIONS BEFORE COMPLETING FORM
1. REPORT NUMBER ESL-TR-82-50	2. GOVT ACCESSION NO. AD-A137244	3. RECIPIENT'S CATALOG NUMBER
4. TITLE (and Subtitle) Evaluation of NASA Structural Analysis (NASTRAN) to Predict the Dynamic Response of Reinforced Concrete	5. TYPE OF REPORT & PERIOD COVERED Final Report 27 May 1981 - 5 Aug 1981	
	6. PERFORMING ORG. REPORT NUMBER	
7. AUTHOR(s) Payne, William W., Jr.	8. CONTRACT OR GRANT NUMBER(s) F49620-79-C-0038	
9. PERFORMING ORGANIZATION NAME AND ADDRESS Headquarters, Air Force Engineering and Services Center (AFESC), Tyndall AFB FL 32403	10. PROGRAM ELEMENT, PROJECT, TASK AREA & WORK UNIT NUMBERS PE 62601F JON: 26730003	
11. CONTROLLING OFFICE NAME AND ADDRESS Headquarters, Air Force Engineering and Services Center (AFESC), Tyndall AFB FL 32403	12. REPORT DATE December 1983	
	13. NUMBER OF PAGES 47	
14. MONITORING AGENCY NAME & ADDRESS (if different from Controlling Office)	15. SECURITY CLASS. (of this report) UNCLASSIFIED	
	15a. DECLASSIFICATION/DOWNGRADING SCHEDULE	
16. DISTRIBUTION STATEMENT (of this Report)  Distribution Unlimited: Approved for Public Release.		
17. DISTRIBUTION STATEMENT (of the abstract entered in Block 20, if different from Report)		
18. SUPPLEMENTARY NOTES  Availability of this report is specified on reverse of Front Cover.		
19. KEY WORDS (Continue on reverse side if necessary and identify by block number) Dynamic Analysis Finite Element Analysis NASTRAN Reinforced Concrete Structural Analysis		
20. ABSTRACT (Continue on reverse side if necessary and identify by block number) This report evaluates the ability of the finite element program, NASTRAN, to analyze reinforced concrete structures under dynamic loads. Experimental data from a quarter scale model test of an underground shelter was used to validate the computer projections.  NASTRAN is a general-purpose structural analysis program containing several types of finite elements and several displacement analysis approaches.		

DD FORM 1 JAN 73 1473

EDITION OF 1 NOV 65 IS OBSOLETE

UNCLASSIFIED

SECURITY CLASSIFICATION OF THIS PAGE (When Data Entered)

For this study five different computer models of reinforced concrete were used. The models were composed of the following elements:

1. Plate membrane elements,
2. Plate membrane and rod elements.
3. Plate-bending elements.
4. Plate-bending-membrane elements.
5. Plate-bending-membrane and beam elements.

Static Analysis and Transient Analysis approaches were used to evaluate the computer model.

Favorable results were obtained for the plate membrane and rod element model using the Transient Analysis Approach. Strain in the reinforcing rods, time to maximum strain, and time to return to zero strain were used to compare the experimental data to the computer prediction.

## PREFACE


This report documents the work accomplished during the USAF Summer Faculty Research Program (1981) by the Southeastern Center for Electrical Engineering Education (SCEEE), 1101 Massachusetts Ave., St. Cloud, FL 32769 under USAF Contract Number F49620-79-C-0038. This contract is sponsored by the Air Force Office of Scientific Research, Air Force Systems Command, Bolling AFB, Washington, DC and was accomplished at the Air Force Engineering and Services Center, Engineering and Services Laboratory, (AFESC/RD) Tyndall AFB, FL.

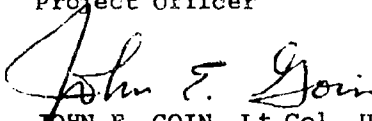
This is a reprint of a report previously published by SCEEE in the 1980 USAF/SCEEE Summer Faculty Research Program, Research Reports Volume I, and covered the period between 27 May 1981 and 5 August 1981. Captain Paul L. Rosengren, Jr. was the AFESC/RDCS project officer.

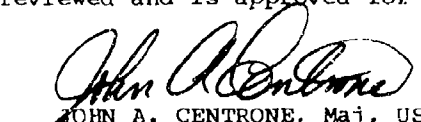
The author would like to express his appreciation to the Air Force Engineering and Services Center, the Engineering Research Division, Airbase Survivability Branch, and the Southeastern Center for Electrical Engineering Education for the opportunity to participate in the 1981 Summer Faculty Research Program and the personnel of the Airbase Survivability Branch for their hospitality to him and his family, and the excellent working conditions the branch members provided. Special credit is given to Mr. David R. Colthorp, Structural Mechanics Division, Waterways Experiment Station, for performing the scale model testing and supplying the experimental results.


This report have been reviewed by the Public Affairs Office (PA) and is releasable to the National Technical Information Service (NTIS). At NTIS it will be available to the general public, including foreign nationals.

This technical report has been reviewed and is approved for publication.

  
PAUL L. ROSENGREN, JR., Capt, USAF  
Project Officer

  
JOHN E. GOIN, Lt Col, USAF  
Chief, Engineering Research Division

  
JOHN A. CENTRONE, Maj, USAF  
Chief, Airbase Survivability Branch

  
ROBERT E. BRANDON, Deputy  
Director, Engineering & Services  
Laboratory

Approved for	
NTIS	
178877	
Unannounced	
Classification	



# TABLE OF CONTENTS

Section	Title	Page
I	INTRODUCTION.....	1
II	OBJECTIVES.....	2
III	FINITE ELEMENT MODELS AND RESULTS.....	3
	PLATE MEMBRANE MODEL.....	5
	PLATE MEMBRANE AND ROD MODEL.....	5
	PLATE-BENDING MODEL.....	7
	PLATE-BENDING - MEMBRANE MODEL.....	7
	PLATE-BENDING - MEMBRANE AND BEAM MODEL.....	8
IV	CONCLUSIONS.....	9
V	RECOMMENDATIONS.....	10
	REFERENCES.....	12
Appendix		
A	FIGURES.....	15
B	TABLES.....	22
C	DISPLACEMENT APPROACH RIGID FORMATS.....	36
D	NASTRAN FINITE ELEMENTS.....	40
E	QUARTER-SCALE UNDERGROUND SHELTER TEST.....	43
F	RESISTANCE - DEFLECTION FUNCTIONS.....	47

# LIST OF FIGURES

Figure	Title	Page
A-1	Undeformed Shape for Membrane and Membrane Rod Finite Element Models.....	16
A-2	Undeformed Shape for Plate-Bending and Plate-Bending-Beam Finite Element Models.....	17
A-3	NASTRAN Plot of Deformed Membrane Model.....	18
A-4	NASTRAN Plot of Deformed Plate-Bending Model.....	19
A-5	Typical NASTRAN Stress vs Time Plot.....	20
A-6	Typical NASTRAN Deflection vs Time Plot.....	21

# LIST OF TABLES

Table	Title	Page
B-1	MEMBRANE FINITE ELEMENT (QDMEM2) MODEL VS TEST 1 RESULTS FOR GAGE ET4.....	23
B-2	MEMBRANE FINITE ELEMENT (QDMEM2) MODEL VS TEST 1 RESULTS FOR GAGE ET5.....	24
B-3	MEMBRANE-ROD FINITE ELEMENT (QDMEM2, ROD) MODEL VS TEST 1 FOR GAGE ET4.....	25
B-4	MEMBRANE-ROD FINITE ELEMENT (QDMEM2, ROD) MODEL VS TEST 1 FOR GAGE ET5.....	26
B-5	MEMBRANE-ROD FINITE ELEMENT (QDMEM2, ROD) MODEL VS TEST 1 FOR GAGE ET4.....	27
B-6	MEMBRANE-ROD FINITE ELEMENT (QDMEM2, ROD) MODEL VS TEST 1 FOR GAGE ET5.....	28
B-7	MEMBRANE-ROD FINITE ELEMENT (QDMEM2, ROD) MODEL VS TEST 1 FOR GAGE ET3.....	29
B-8	MEMBRANE-ROD FINITE ELEMENT (QDMEM2, ROD) MODEL VS TEST 1 FOR GAGE ET2.....	30
B-9	MEMBRANE-BENDING FINITE ELEMENT (QUAD1) MODEL VS TEST 1 RESULTS FOR GAGE ET4.....	31
B-10	MEMBRANE-BENDING FINITE ELEMENT (QUAD1) MODEL VS TEST 1 RESULTS FOR GAGE ET5.....	32
B-11	MEMBRANE-BENDING AND ROD FINITE ELEMENT (QUAD1, BAR) MODEL VS TEST 1 RESULTS FOR GAGE ET4.....	33
B-12	MEMBRANE-BENDING AND ROD FINITE ELEMENT (QUAD1, BAR) MODEL VS TEST 1 RESULTS FOR GAGE ET5.....	34
B-13	MATERIAL AND SECTION PROPERTIES FOR QUARTER-SHELL MODEL.....	35

## SECTION I

### INTRODUCTION

The United States Air Force is investigating ways of predicting the response of reinforced concrete in hardened structures due to blast (dynamic) loads. The dynamic loads are caused by the nearby explosion of conventional (non-nuclear) weapons. Current-generation hardened structures are reinforced concrete construction, covered with layer(s) of soil, rock rubble, and/or a burster slab. The structures have boxy shapes with heavily reinforced concrete walls, floors, and roofs.

The Air Force hopes to reduce the costs of construction by improving the analysis and design techniques. Substantial savings can be made by reducing the amount of steel required in the shelters.

Present design and analysis procedures use "limit-state" theory to determine the ultimate strength of the structure and idealize the structure as a single degree-of-freedom system to predict the required resistance. These assumptions neglect the interaction between the structural components such as the roof and the supporting walls. Finite element techniques offer the best means of modeling the structural interaction between components and predicting the capacity of each component.

Commonly available structural analysis programs are not strictly applicable to this problem. Most programs do not contain nonlinear material behavior and provisions for soil elements, concrete-soil interaction, or steel-concrete interaction. The few programs that address these areas are designed for nuclear weapons where the loading has a long-duration shock front. Conventional weapons have a short-duration pressure wave that decreases rapidly with distance from the detonation (Reference 1).

Many current investigations attempt to accurately model reinforced concrete for use in finite element programs. Investigators are developing models of the concrete that will exhibit the nonlinear stress-strain behavior and the low tensile strength that result in cracking and loss of stiffness in the reinforced concrete. More sophisticated models are including strain-rate effects and load histories so that repeated detonations can be modeled (Reference 2). Present design criteria for hardened structures do not call for repeated explosions from conventional weapons.

Besides the modeling problems of concrete, the interaction between the reinforcing steel and concrete is not completely understood. An accurate reinforced concrete element must model the bond stress and friction from interlocking between the deformed reinforcing bars and the concrete.

Until a complete reinforced concrete model is developed, analysis techniques will be able to predict failure mechanisms related to the response of the complete structure only. For those explosions where the structure can respond as a unit, developing bending and membrane forces, finite element methods can model the response with sufficient accuracy. Structural response where the pressures are high enough to cause failure of a localized area can not be modeled (Reference 1).



## SECTION II

### OBJECTIVES

The main objective of this project was to determine if the finite element program, NASTRAN, is a useful tool in modeling the response of hardened reinforced concrete structures. The accuracy of the finite element model was of primary importance and results from tests on a quarter-scale model of an underground structure were used to evaluate the computer predictions. The utility of the program was also judged on the usefulness of the output and the ease of input.

A secondary objective was to understand the full capabilities of NASTRAN and to relate them to the problems associated with modeling reinforced concrete. This would identify areas of NASTRAN that could be changed to improve its ability to model reinforced concrete.

### SECTION III

#### FINITE ELEMENT MODELS AND RESULTS

NASTRAN (NASA Structural Analysis) was developed to aid in the linear analysis of structures for the loading conditions associated with flight. Different static and dynamic analysis approaches are available and limited nonlinear capability is included. Nonlinear behavior may arise from changes in geometric shape or material properties.

To evaluate NASTRAN, different finite element models of a quarter-scale underground shelter were constructed and used in different static and dynamic analysis approaches. The finite element models were representative of the element types available in NASTRAN and were not intended to be sophisticated models of reinforced concrete, since an accurate reinforced concrete element does not exist. The models used were a combination of rod and plate elements in which the rods represented the reinforcing steel and the plates represented the concrete and a plate element alone that modeled both the steel and concrete.

The models were used in different analysis approaches and the predictions compared to the recorded data from the actual test. The computer projections were output in numerical and graphical form and the usefulness of the output was evaluated. Because of the limited experimental data, the model predictions for maximum strain at specific locations of reinforcing steel, time to that maximum strain, and time to return to zero strain were used to judge the accuracy of the model.

The points used for evaluation were located on the top layer of reinforcing steel at the middle of the roof span and at the face of the interior wall (see Figure A-1). The gage points are denoted by ET4 and ET5 for Test 1 and by ET2 and ET3 for Test 2. These points had the best experimental records for both Test 1 and Test 2.

A better measure of the accuracy of the model would have been deflections rather than strains. However, deflection data were unavailable. For the model composed of plates only, strain output from NASTRAN was not possible and some bias was introduced when converting deflections to strain.

The finite element models were used in two displacement analysis approaches, static and transient. The static approach used the static "equivalent" uniform loads provided in Reference 4. No mass effects are considered in static analysis. This analysis was used to develop a resistance-deflection function for each finite element model.

The transient analysis used a linear representation of the load history taken from the pressure-time traces in Reference 4. A grid point was placed at each pressure gage location (see Figure A-7) for each finite element model. The loads could be applied directly to each grid point by assuming the

pressure was uniformly distributed over one-half the element length in both directions. The loads were stopped at the face of each wall.

Because the transient approach is a dynamic analysis, structural damping and nonstructural mass effects of the covering soil and burster slab can be included, using NASTRAN. For this investigation, they were omitted, except for the model composed of plate membrane and rod finite elements. Varying amounts of damping and nonstructural mass were added to the model to determine their effects. Damping and nonstructural mass were applied independently of each other.

No rational way of predicting the amount of structural damping is available, so the amounts used were chosen in an attempt to fine-tune the model. The denominator in the damping coefficient fraction is the second natural frequency from an eigenvalue analysis and the numerator was chosen to improve model response. A convenient way of converting this damping to percentage of critical damping was not found.

Some of the mass above the shelter roof acts with the roof and therefore affects the mass terms in the dynamic equilibrium equation. The nonstructural mass of the concrete burster slab, plus the covering soil and the nonstructural mass of the soil only, was placed on the roof of the model. Since there is no way of determining how much nonstructural mass acts with the shelter, these two amounts seem to be the logical choices.

The effects of damping and nonstructural mass were added to the Transient Analysis Approach on a model that included nonlinear loads. All NASTRAN dynamic approaches assume linear material properties. As the stress in the concrete increases, the concrete cracks in the tension zone and responds nonlinearly in the compression zone. Presently, the only way of inducing nonlinear behavior in the NASTRAN dynamic approaches is by including loads triggered by the displacements and/or velocities of grid points.

To represent the loss of stiffness in a reinforced concrete member due to cracking; nonlinear loads based on the resistance deflection function were applied in the direction of the blast loading. The load was equal to the difference between the NASTRAN elastic prediction (static analysis) for the resistance-deflection function and the resistance-deflection function as described in Reference 10. A detailed description of the resistance-deflection function is found in Appendix F.

The additional load used was assumed to start at the deflection where the finite element model strength and the ultimate moment strength from Reference 10 coincided. The load increased linearly to the maximum deflection of the shelter. This neglected the portion of the resistance-deflection function, whereas the finite element model underestimated the flexural strength of the reinforced concrete structure.

The finite element models require certain geometric and material properties. Table B-13 contains the section properties of the quarter-scale model.

Appendices C and D contain brief discussions of the NASTRAN analysis approaches and finite elements. The discussions deal only with those parts of the approaches and elements applicable to modeling reinforced concrete under blast loadings. More detailed information is available in References 12 and 13. Appendix E describes the quarter-scale model.

#### PLATE MEMBRANE MODEL

The initial model was composed of plate membrane elements (QDMEM2) representing both the steel and the concrete. The model was formed by passing two parallel planes a unit distance apart through the cross section of the shelter (See Figure A-1). The nodes of each element were on the outermost concrete fiber, halfway between the planes. No attempt was made to model the reinforcing steel, and the concrete material properties were used for all elements.

For this element, output of strain at the location of the reinforcing steel was not available. The difference in the horizontal displacements was converted to strain by dividing by the length of the elements. This was the strain on the outermost top and bottom concrete fibers. By assuming plane sections remain plane, these strains were converted to strain at the location of the reinforcing steel by using similar triangles. Since the grid mesh is very coarse, this strain was a crude average. In the Transient Analysis Approach, the time to maximum strain and the time to return to zero strain were assumed to occur at the time to maximum horizontal displacement, and at the time to return to zero horizontal displacement, respectively.

The results from this model are in Tables B-1 and B-2. The maximum strain in the static and transient approaches is too small, particularly near the interior wall, and the time to zero strain is much too short for the transient approach. Nonlinear loads increase the strains and the time to return to zero strain; however, the loads did not improve the overall accuracy of the model.

The results from this model do not indicate that membrane elements alone could successfully model a reinforced concrete shelter under blast loads. The structure has a thick roof with very short spans, so that inplane forces are predominant. If membrane elements alone could model a hardened shelter, they should work for this particular structure. As the vertical deflections increase or as the span of the roof lengthens, bending would become more important and the membrane model would become worse.

#### PLATE MEMBRANE AND ROD MODEL

To improve the representation of reinforced concrete, rod elements (ROD) with linear steel properties were added to the membrane finite elements. The

nodes for the membrane and rod elements were moved to the location of the reinforcing bars. An advantage of this model over the plate membrane model alone, is that although many new elements were added, the solution times should not be substantially increased because no additional nodes were added. The membrane elements represent the concrete between the top and bottom reinforcement. This neglects the concrete in compression outside the steel bars; however, it includes the portion of the concrete in tension between the reinforcing steel layers.

This model worked very well up to the maximum strain using a transient analysis approach (see Tables B-3 and B-4). The percentage difference for the maximum strain and the time to maximum strain were small enough to be considered negligible. Even when the most sophisticated methods are used to determine material properties, the coefficient of variation for deflection predictions is in the order of 15 to 20 percent (reference 3). For this case, the worse percentage difference (31 percent) should be considered excellent.

Since the results for Test 1 loads were so good, this model was used with the loads from Test 2. Results were excellent except for the maximum strain at the middle of the roof span (Table B-8, Gage ET2). The experimental results for this gage are questionable. Normally, the first plastic hinge would form at this point and this section would have the largest strain in the roof. Therefore, the computer model is probably more accurate than shown in Table B-8.

Nonlinear loads decreased the accuracy of the model by causing too much increase in maximum strain and the time to maximum strain. Strain was improved.

The effects of nonstructural mass were investigated using this model and the results are presented in Tables B-3 and B-4. The amount of strain was greatly reduced and the response time of the structure increased. Even with only the weight of the soil applied to the roof, the model was much too stiff and slow to respond. A small amount of nonstructural mass could improve the response of the model; however, a rational way of determining the nonstructural mass is not available.

This model was also used to test the effects of structural damping. The results are shown in Tables B-5, B-6, B-7, and B-8. As the structural damping increased, the maximum strain and the time to maximum strain decreased, and the time to return to zero strain increased. Although the amount of damping was chosen in an attempt to fine-tune the model, the results were no better than in the transient approach without nonlinear loads.

This model works particularly well up to the point of maximum strain. Beyond that time the model responds too quickly. By including the proper amount of structural damping and nonstructural mass the model response could be improved for a longer time period.

## PLATE-BENDING MODEL

A model was made of the shelter using plate-bending elements (QDPLT) only. The model is formed by passing two parallel planes 12 inches apart through the shelter cross section. The nodes of the elements are on the middle surface of the walls, roof, and floor (see Figure A-2). The material properties used were for concrete. Bigg's moment of inertia for a cracked reinforced concrete section was used for the bending stiffness. The distance from the compression face to the centroid to the tension steel was used as the transverse shear thickness (Reference 2).

The model was used in a static analysis approach only, because the elements require unrealistic boundary conditions. A plate-bending element cannot resist inplane forces, so to be used as an element in a wall the vertical deflection of the wall must be completely constrained. Other finite elements do not require such restrictive boundary conditions and are more useful. This element may be employed as a roof element when used in combination with other element types. The roof should have a large span-to-depth ratio.

## PLATE BENDING-MEMBRANE MODEL

By using an element that can develop inplane forces, realistic boundary conditions can be used. A model using plate-bending-membrane finite elements (QUAD1) was constructed in the same manner as for the plate-bending model. Since the reinforcing steel was not being modeled, concrete material properties were used. Bigg's moment of inertia was used for bending stiffness, the distance from the compression face to the centroid of the tension steel was used for the transverse shear thickness, and the total concrete thickness was used for the membrane shear thickness (Reference 2).

For the accuracy required to analyze or design a shelter, the plate-bending membrane model requires approximately the same number of nodes as a plate-membrane element model. Because of the gross mesh size used in this project, extra nodes had to be added for the plate-bending-membrane model. The stresses in each element are an average of the stresses within the element. This caused the element at the face of the interior wall to have small tensile strains rather than the large compression strains expected. Placing a small element at the face of the wall (see Figure A-2) corrected this problem.

Tables B-9 and B-10 contain the results from the Static and Transient Analysis Approaches. The model is too flexible, does not reach the maximum strain soon enough, and returns to zero strain too quickly. Nonlinear loads worsen the predictions, as would be expected for an overly flexible model.

A model composed of plate-bending-membrane elements alone did not exhibit the kinds of characteristics necessary to model reinforced concrete. The flexibility of the model depends on the designer's choice for a moment of inertia. Also, input values for the transverse shear and membrane shear thickness are debatable. A better finite element model would have fewer and less critical choices.

## PLATE BENDING - MEMBRANE AND BEAM MODEL

By adding a beam (BAR) element to the bending-membrane model the importance of the value of the moment of inertia is reduced. The plate element was used to represent the concrete and was given concrete material properties. The bending stiffness was the moment of inertia of the concrete between the center of gravity of the total section and the top layer of steel about the center of gravity of the total section (neglects concrete outside the steel layer). The transverse shear thickness was the distance from the compression face to the centroid of the tension steel and the membrane shear thickness was the distance between the steel layers.

Two beam elements were offset the proper distance in each direction, on each side of the middle surface of the plate. By releasing the the proper constraints only axial extension of each beam was allowed and bending was eliminated. Each beam had a cross-sectional area equal to one-half the reinforcing steel area in each layer and each element had the standard steel material properties.

The results from this model are in Tables B-11 and B-12. The model works well in a Transient Analysis Approach, without nonlinear loads. Good results are obtained at the midspan of the roof; where bending forces are predominant. Applying nonlinear loads increased the maximum strain and increased the time to maximum strain; however, it did not improve the overall accuracy of the model. Near the interior support the model was too stiff, even with nonlinear loads applied. As with all models, this one returned to zero strain much too quickly.

The plate bending-membrane and beam model was the second most accurate model in this investigation. Indications are the model would be more accurate for longer span, thinner roof sections. The depth-to-span ratio of 3/16 is not small deflection plate theory and this model may be more applicable to full-size structures (Reference 11). The input requirements for this model are large because of the large number of elements; therefore, significant gains in accuracy would have to be achieved before this would be the model of choice.

## SECTION IV

### CONCLUSIONS

The finite element program NASTRAN can be extremely useful for analyzing and designing hardened reinforced concrete shelters. When using a finite element model composed of plate membrane elements (QDMEM2) and rod elements (ROD), the structure is correctly modeled up to the maximum strain at the roof span centerline and near interior support. Since the strains are accurately modeled, it is reasonable to assume deflections are also successfully predicted.

Element stresses will not be correct because a linear stress-strain relationship is used by NASTRAN. Element forces are determined directly from the element displacement matrix and will be as accurate as the displacements. Deflection predictions of reinforced concrete members traditionally have a large degree of uncertainty and a prediction within 20 percent of the true deflection should be considered excellent (Reference 3). The large prediction error is related to material property and construction practices, so reductions in the size of the error cannot be made by improving the mathematical modeling techniques.

Better modeling techniques will help improve the deflection predictions for repeated explosions for pressures high enough to cause localized failures, and for time intervals that exceed the time to maximum strain. In particular, better techniques are needed to predict permanent set of a hardened structure. The areas that need improvement are in the finite element representation of reinforced concrete, the amount and type of structural damping in hardened structures, and the amount of covering material that acts as nonstructural mass on the roof.

When dynamic analysis of a hardened structure is conducted, huge amounts of output data are generated. By far the most functional form of output is graphical. Numerical output inundates the engineer with data and does not provide a feeling for how the structure is responding. The graphical capabilities of NASTRAN are a tremendous advantage. Undeformed plots (see Figures A-1 and A-2) and deformed plots (see Figures A-3 and A-4) may be made separately or superimposed. Plots of elements stresses, strains and forces versus time (see Figure A-5) and plots of grid point deflections, velocities, and accelerations versus time (see Figure A-6) are available. Input loads versus time also can be plotted (Reference 13).

Input for NASTRAN is tedious at best. A large number of cards must be punched for small problems and the number increases quickly as the number of elements increase. The format of the input cards is rigid, with input data restricted to certain fields. Where interactive computer service is available, input data could be written to disk as card images and properly formatted by simple user-written programs. This relieves some of the monotony of inputting data but would not reduce the number of characters input.



## SECTION V

### RECOMMENDATIONS

Results from the analyses performed during this project indicate NASTRAN in its present form is useful in analyzing hardened reinforced concrete shelters up to the time of maximum strain. The test used in this project had a limited amount of useful data. More validation runs of NASTRAN should be made before the program is used for design of hardened structures. The test data needed for the validation run are:

- (1) blast pressures on the surface of the reinforced concrete member(s).
- (2) deflections and velocity of regularly spaced points on the outer surfaces of the reinforced concrete member(s).
- (3) strains at selected points on the tension and compression steel.

The boundary conditions on the test specimen should be instrumented so that any support movement can be determined and used in the analytic model. Any strain gage used on a concrete surface should use at least 3 inches of length to eliminate bias from cracks and coarse aggregates.

The ability of NASTRAN to model reinforced concrete can be improved by adding nonlinear material behavior to the dynamic analysis approach. Nonlinear material behavior is available in a static approach (Piecewise Linear Analysis) and could be added to the dynamic approaches by changing the rigid formats.

Accurate prediction of structural response beyond the maximum strain requires basic research into the nature of structural damping and nonstructural mass. The limited analytic study in this project showed the computer model to be very sensitive to changes in nonstructural mass and structural damping. The surrounding and covering soil layers (including burster slab) act with the shelter as nonstructural mass and add structural damping. Since both phenomena are related, a nondimensional model study may be able to develop rational methods of determining structural damping and nonstructural mass for the specific configuration of a hardened structure (Reference 9).

Intensive work is being done developing a reinforced concrete finite element and a good element should be available at any time (Reference 5). Most work is being done to model nuclear explosions and the finite element will have to be changed to properly model reinforced concrete subjected to a conventional weapon explosion. Whenever the model becomes available, it should be added to NASTRAN to improve its ability to predict the response of reinforced concrete structures.

The new element will contain strain/rate (or stress/rate) effects on material properties. Most of the data available on strain/rate effects are 23 years old or older and contain some questionable data. However, the information indicates gains in ultimate concrete strength are in the range 50 to 100 percent (References 6, and 7). An investigation into the strain/rate effect is needed and should lead to substantial cost savings in reinforced concrete shelters.

Investigation into the use of other general purpose finite element programs should continue. Emphasis should be given to those programs that contain dynamic analysis capabilities that include structural damping and non-structural mass. The programs should be able to be altered to take new finite elements. A most important consideration is the ability to generate graphical output. Lack of graphical output would seriously affect the program's ability for practical use.

## REFERENCES

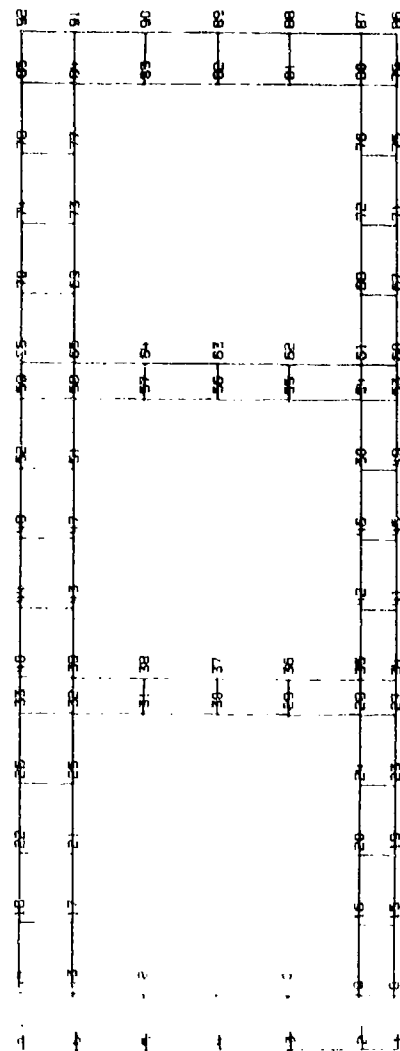
1. Baseheart, T. M., The Response of Reinforced Concrete Structures to Near Field Explosions, USAF Summer Faculty Research Program, Vol 1, AFOSR, Bolling AFB, Washington, DC, 1980.
2. Hegemier, G. A., Evaluation of Material Models for MX Siting Vol II: Reinforced Concrete Models, SSS-R-80-4155, Systems, Science and Software, LaJolla, CA, November 1979.
3. Biggs, J. M., Introduction to Structural Dynamics, McGraw-Hill Book Co, New York, NY, 1964.
4. Branson, D. E., Deformation of Concrete Structures, McGraw-Hill Book Co, New York, NY, 1977.
5. Coltharp, D. A., Analysis of One-Quarter-Scale Model Test Results, Unpublished Report from USA Waterways Experiment Station, Structures Laboratory, Structure Mechanics Division, Vicksburg, MS.
6. Mindess, S., and Young, J. F., Concrete, Prentice-Hall, Inc., Englewood Cliffs, NJ, 1981.
7. Neville, A. M., Properties of Concrete, Pitman Publishing Limited, London, Great Britain, 1981.
8. Przemieniecki, J. S., Theory of Matrix Structural Analysis, McGraw-Hill Book Co., New York, NY, 1968.
9. Smith, J. H., and Vann, W. P., Theoretical and Experimental Investigation of Buried Concrete Structures Vol I: Analysis and Experiment, AFOSR-TR-76-1070, AFOSR, Bolling AFB, Washington, DC, November 1975.
10. Structures to Resist the Effects of Accidental Explosions, AFM88-22, Departments of the Army, the Navy, and the Air Force, Washington, DC, June 1969.
11. Szilard, R., Theory and Analysis of Plates, Prentice-Hall, Inc., Englewood Cliffs, NJ, 1974.
12. The NASTRAN Theoretical Manual, NASA SP-221(05), National Aeronautics and Space Administration, Washington, DC, December 1980.
13. The NASTRAN User's Manual, NASA SP-222(05), National Aeronautics and Space Administration, Washington, DC, December 1980.
14. Timoshenko, S. P., and Goodier, J. N., Theory of Elasticity, McGraw-Hill Book Co., New York, NY, 1934.

15. Venkayya, V. B., Eastep, F. E., and Johnson, J. R., NASTRAN Beginner's Course, TM-FBR-76-121, Air Force Flight Dynamics Laboratory, Wright-Patterson AFB, OH, September 1976.

16. Wang, C. K., and Salmon, C. J., Reinforced Concrete Design, Harper and Row Publishers, New York, NY, 1979.

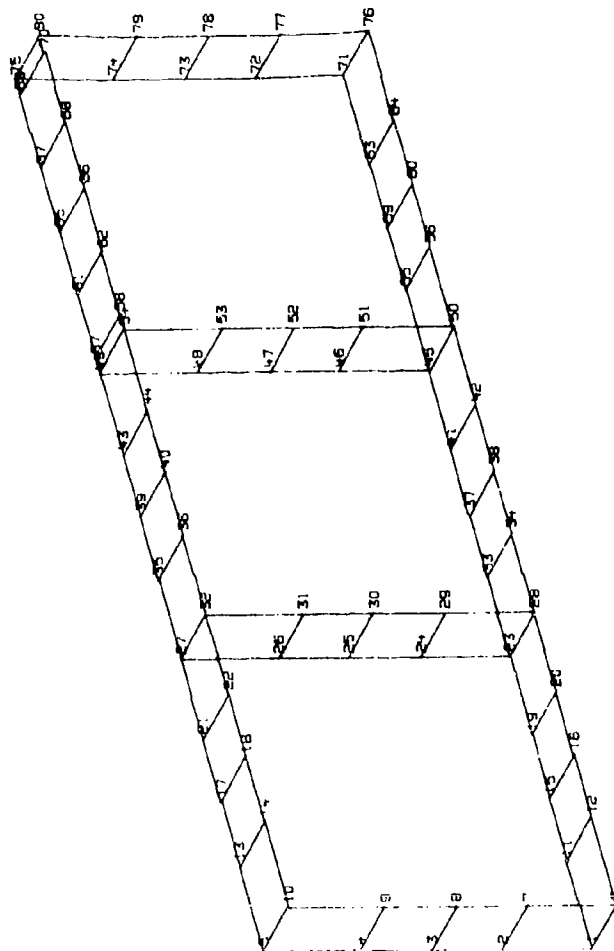
APPENDIX A

FIGURES



STATIC ANALYSIS MEMBRANE ELEMENTS  
 1/4" CONCRETE MATERIAL, GROSS SECTION PROPERTIES  
 UNDEFORMED SHAPE

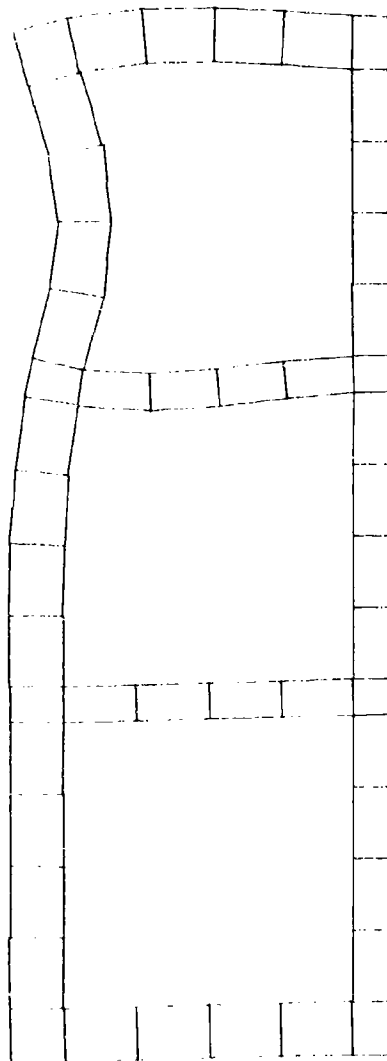
FIGURE A-1. Undeformed Shape For Membrane and Membrane-Rod Finite Element Models



TRANSIENT ANALYSIS - BENDING - MEMBRANE AND BEAM ELEMENTS  
 LINEAR STEEL AND CONCRETE MATERIAL  
 UNDEFORMED SHAPE

FIGURE A-2. Undeformed Shape For Plate Bending and Plate-Bending-Beam Finite Element Models

WAVELENGTH = 0.0005

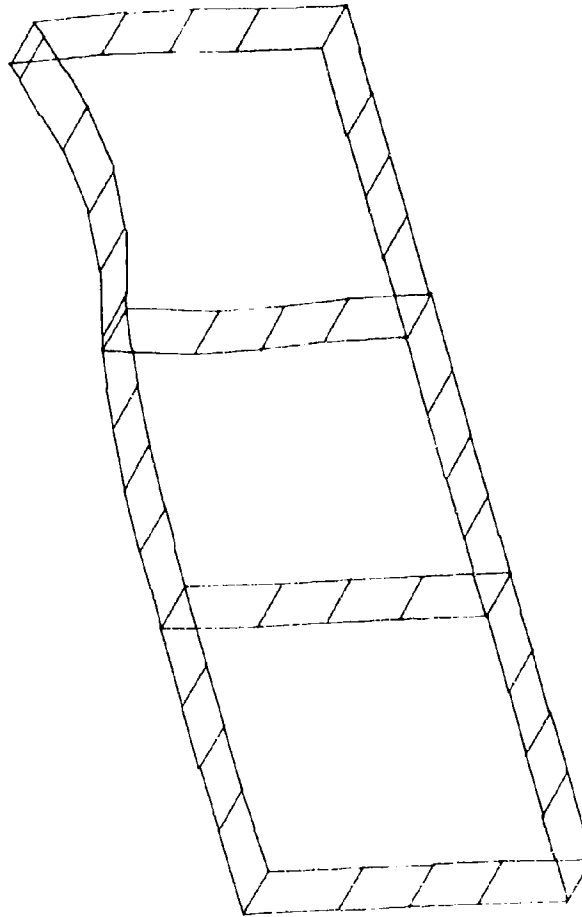


STATIC ANALYSIS MEMBRANE ELEMENTS  
LINEAR CONCRETE MATERIAL, GROSS SECTION PROPERTIES  
GROSS TEST 1 AVERAGE PRESSURE = 1825 PSI  
STATIC DEFOR. SUBCASE 1 LOAD

FIGURE A-3. NASTRAN Plot of Deformed Membrane Model



MAX-DEF. = 0.28099108



STATIC ANALYSIS BENDING - MEMBRANE ELEMENTS AND BEAM  
ELEMENTS LINEAR STEEL AND CONCRETE MATERIAL  
GLCH TEST 1 AVERAGE PRESSURE = 182'S PSI  
STATIC DEFOR. SUBCASE 1 LOAD 1

FIGURE A-4. NASTRAN Plot of Deformed Plate-Bending Model

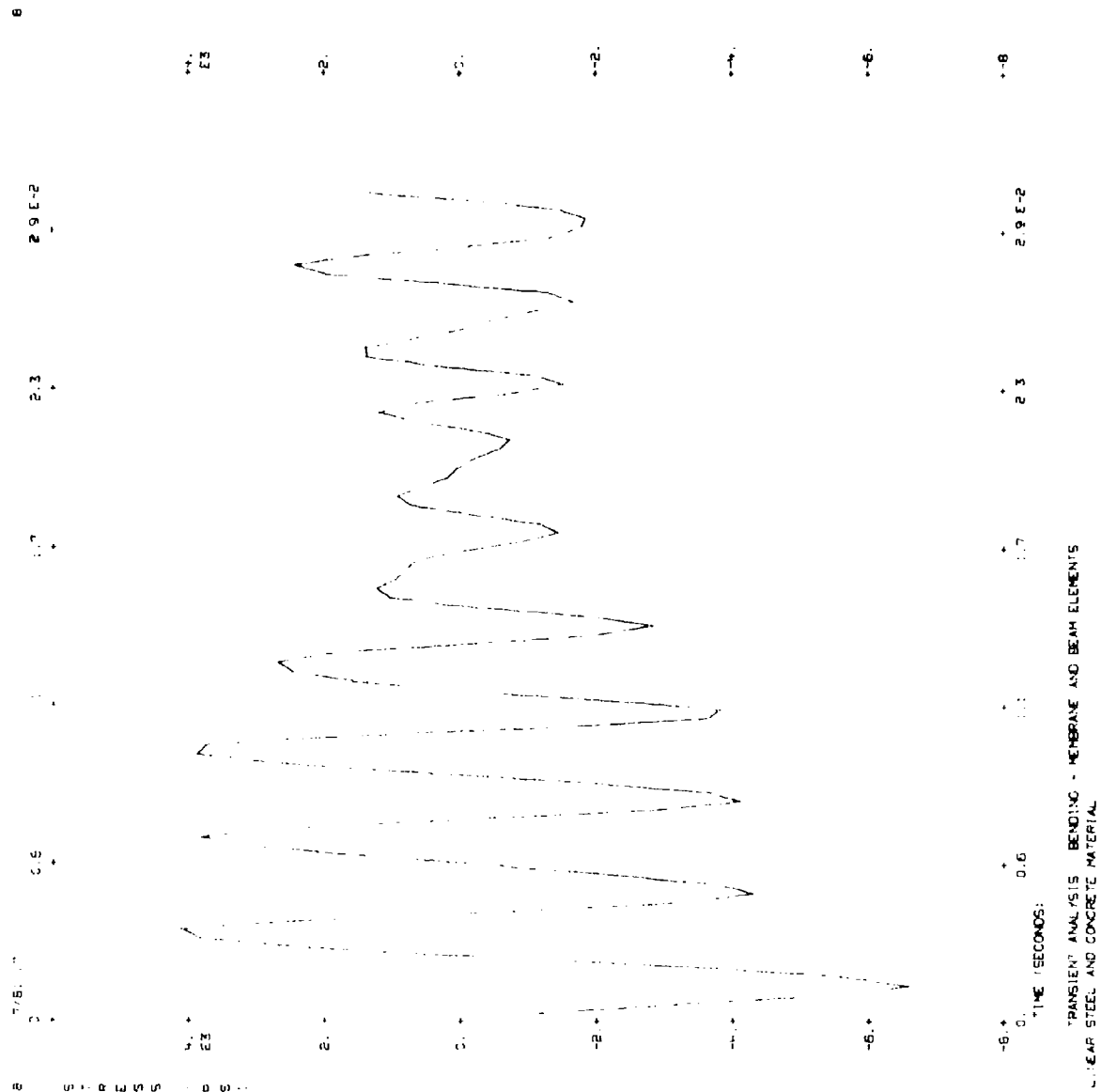
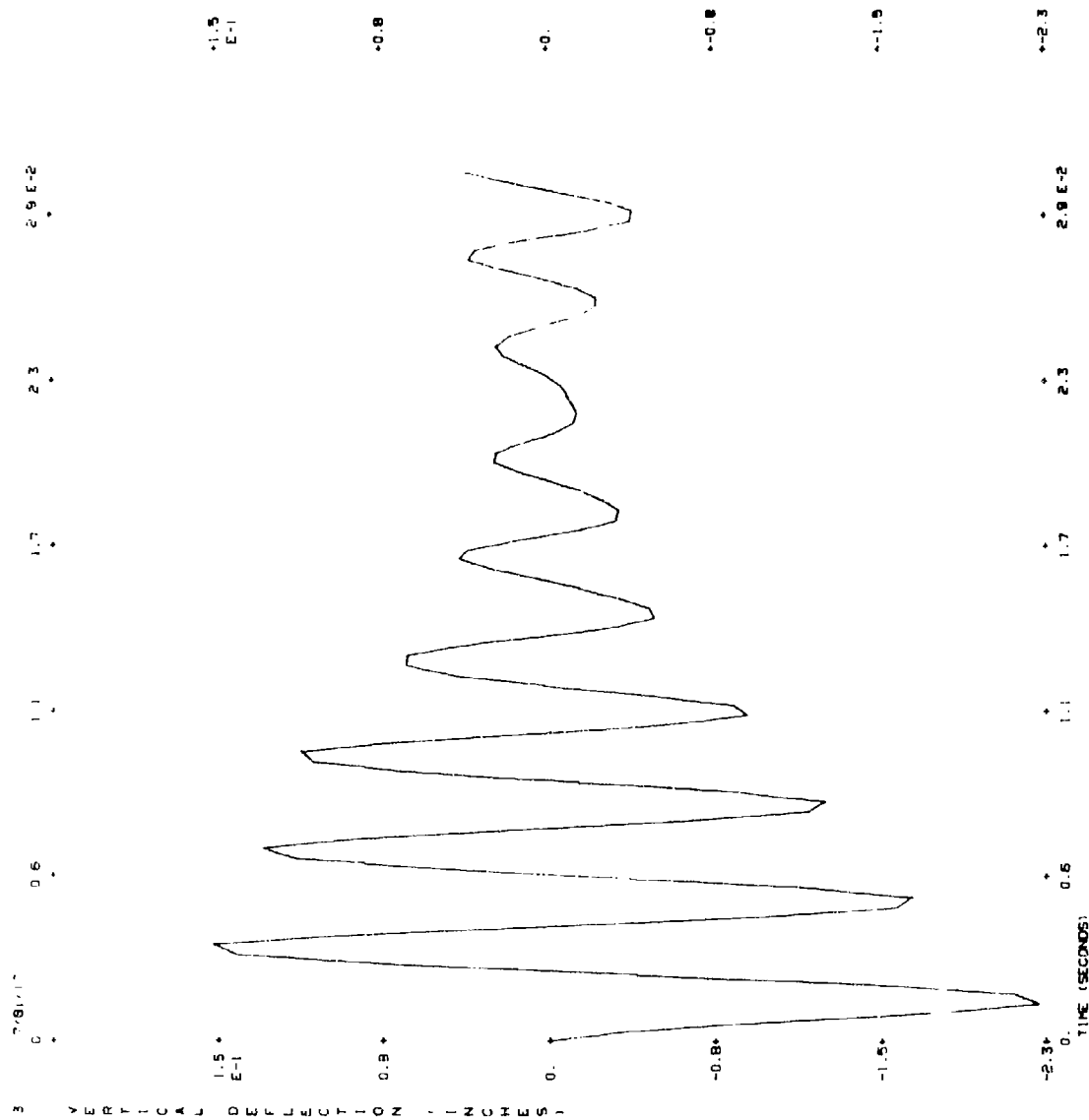


FIGURE A-5. Typical NASTRAN Stress vs Time Plot



TRANSIENT ANALYSIS BENDING - MEMBRANE AND BEAM ELEMENTS  
 LINEAR STEEL AND CONCRETE MATERIAL

FIGURE A-6. Typical Nastran Deflection vs Time Plot

APPENDIX B

TABLES

TABLE B-1. MEMBRANE FINITE ELEMENT (QDMEM2) MODEL  
VS TEST 1 RESULTS FOR GAGE ET4

ANALYSIS TYPE	Experimental	Static	Transient	Transient 1
MAXIMUM STRAIN & DIFFERENCE	$1750 \times 10^{-6}$	$1100 \times 10^{-6}$ -37%	$1050 \times 10^{-6}$ -40%	$2410 \times 10^{-6}$ 37%
TIME TO MAXIMUM STRAIN (SEC) & DIFFERENCE	$2.5 \times 10^{-3}$	N/A	$2.9 \times 10^{-3}$ 18%	$4.0 \times 10^{-3}$ 60%
TIME TO ZERO STRAIN (SEC) & DIFFERENCE	$8.5 \times 10^{-3}$	N/A	$4.1 \times 10^{-3}$ -52%	$5.4 \times 10^{-3}$ -36%

Notes:  
Transient 1: Includes nonlinear loads

TABLE B-2. MEMBRANE FINITE ELEMENT (QDMEM2) MODEL  
VS TEST 1 RESULTS FOR GAGE ETS

ANALYSIS TYPE	Experimental Test	Static	Transient	Transient 1
MAXIMUM STRAIN & DIFFERENCE	$-2100 \times 10^{-6}$	$-2090 \times 10^{-6}$ -1%	$-2010 \times 10^{-6}$ -4%	$-4150 \times 10^{-6}$ 98%
TIME TO MAXIMUM STRAIN (SEC) & DIFFERENCE	$2.5 \times 10^{-3}$	N/A	$3.0 \times 10^{-3}$ 20%	$4.0 \times 10^{-3}$ 60%
TIME TO ZERO STRAIN (SEC) & DIFFERENCE	$10 \times 10^{-3}$	N/A	$4 \times 10^{-3}$ -60%	$5.4 \times 10^{-3}$ -46%

Notes:

Transient 1: Includes nonlinear loads

TABLE B-3. MEMBRANE-ROD FINITE ELEMENT (QDMEM2, ROD) MODEL  
VS TEST 1 FOR GAGE ET4

ANALYSIS TYPE	Experimental Test	Static	Transient	Transient	Transient	Transient
					5	6
MAXIMUM STRAIN & DIFFERENCE	$1750 \times 10^{-6}$	$1770 \times 10^{-6}$ 1%	$1640 \times 10^{-6}$ -6%	$3700 \times 10^{-6}$ 110%	$950 \times 10^{-6}$ -46%	$820 \times 10^{-6}$ -53%
TIME TO MAXIMUM STRAIN (SEC) & DIFFERENCE	$2.5 \times 10^{-3}$	N/A	$3.0 \times 10^{-3}$	$4.0 \times 10^{-3}$	$6.0 \times 10^{-3}$	$8.2 \times 10^{-3}$
			21%	61%	139%	226%
TIME TO ZERO STRAIN (SEC) & DIFFERENCE	$8.5 \times 10^{-3}$	N/A	$4.2 \times 10^{-3}$	$5.5 \times 10^{-3}$	$10.0 \times 10^{-3}$	$12.4 \times 10^{-3}$
			-51%	-35%	20%	45%

Notes:

Transient 1: Includes nonlinear loads

Transient 5: Includes nonlinear loads and the nonstructural mass of the soil only

Transient 6: Includes nonlinear loads and the nonstructural mass of the burster slab plus soil

TABLE B-4. MEMBRANE-ROD FINITE ELEMENT (QDMEM2, ROD)  
MODEL VS TEST 1 RESULTS FOR GAGE ET5

ANALYSIS TYPE	Experimental Test	Static	Transient	Transient 1	Transient 5	Transient 6
MAXIMUM STRAIN & DIFFERENCE	$-2.100 \times 10^{-6}$	$-2830 \times 10^{-6}$ 35%	$-2760 \times 10^{-6}$ 31%	$-5380 \times 10^{-6}$ 156%	$-1330 \times 10^{-6}$ -37%	$-990 \times 10^{-6}$ -53%
TIME TO MAXIMUM STRAIN (SEC) & DIFFERENCE	$2.5 \times 10^{-3}$	N/A	$2.9 \times 10^{-3}$ 17%	$4.0 \times 10^{-3}$ 60%	$7.1 \times 10^{-3}$ 185%	$8.1 \times 10^{-3}$ 225%
TIME TO ZERO STRAIN (SEC) & DIFFERENCE	$10 \times 10^{-3}$	N/A	$4.0 \times 10^{-3}$ -60%	$5.6 \times 10^{-3}$ -44%	$10 \times 10^{-3}$ 5%	$12.6 \times 10^{-3}$ 26%

Notes:

- Transient 1: Includes nonlinear loads
- Transient 5: Includes nonlinear loads and nonstructural mass composed of soil only
- Transient 6: Includes nonlinear loads and nonstructural mass composed of burster slab plus soil



TABLE B-5. MEMBRANE-ROD FINITE ELEMENT (QDMEM2, ROD)  
MODEL VS TEST : RESULTS FOR GAGE ET4

ANALYSIS TYPE	Experimental Test	Transient 1	Transient 2	Transient 3	Transient 4
MAXIMUM STRAIN % DIFFERENCE	$1750 \times 10^{-6}$	$3700 \times 10^{-6}$ 110%	$3130 \times 10^{-6}$ 79%	$1560 \times 10^{-6}$ -11%	$1150 \times 10^{-6}$ -34%
TIME TO MAXIMUM STRAIN (SEC) % DIFFERENCE	$2.5 \times 10^{-3}$	$4.0 \times 10^{-3}$ 61%	$4.0 \times 10^{-3}$ 60%	$3.4 \times 10^{-3}$ 34%	$2.4 \times 10^{-3}$ 47%
TIME TO ZERO STRAIN (SEC) % DIFFERENCE	$8.5 \times 10^{-3}$	$5.5 \times 10^{-3}$ -35%	$5.4 \times 10^{-3}$ -36%	$5.5 \times 10^{-3}$ -36%	$10.7 \times 10^{-3}$ 26%

Notes:

- Transient 1: Includes nonlinear loads
- Transient 2: Includes nonlinear loads and damping coefficient 0.1/1719.592
- Transient 3: Includes nonlinear loads and damping coefficient 0.5/1719.592
- Transient 4: Includes nonlinear loads and damping coefficient 1.0/1719.592

TABLE B-6. MEMBRANE-ROD FINITE ELEMENT (QMEM2, ROD) MODEL  
VS TEST 1 RESULTS FOR GAGE ET5

ANALYSIS TYPE	Experimental Test	Transient 1	Transient 2	Transient 3	Transient 4
MAXIMUM STRAIN % DIFFERENCE	$-2100 \times 10^{-5}$	$-5380 \times 10^{-6}$ 156%	$-4620 \times 10^{-6}$ 120%	$-2770 \times 10^{-6}$ 32%	$-1750 \times 10^{-6}$ -17%
TIME TO MAXIMUM STRAIN (SEC) % DIFFERENCE	$2.5 \times 10^{-3}$	$4.0 \times 10^{-3}$ 60%	$4.0 \times 10^{-3}$ 58%	$3.8 \times 10^{-3}$ 51%	$3.6 \times 10^{-3}$ 45%
TIME TO ZERO STRAIN (SEC) % DIFFERENCE	$10 \times 10^{-3}$	$5.6 \times 10^{-3}$ -44%	$5.5 \times 10^{-3}$ -45%	$5.5 \times 10^{-3}$ -45%	$10.7 \times 10^{-3}$ 7%

Notes:

- Transient 1: Includes nonlinear loads
- Transient 2: Includes nonlinear loads and damping coefficient 0.1/1719.592
- Transient 3: Includes nonlinear loads and damping coefficient 0.5/1719.592
- Transient 4: Includes nonlinear loads and damping coefficient 1.0/1719.592

TABLE B-7. MEMBRANE-ROD FINITE ELEMENT (QDMEM2, ROD) MODEL  
VS TEST 2 FOR GAGE ET3

ANALYSIS TYPE	Experimental Test	Static	Transient	Transient 1	Transient 2	Transient 3
MAXIMUM STRAIN & DIFFERENCE	$2700 \times 10^{-6}$	$3440 \times 10^{-6}$ 27%	$2970 \times 10^{-6}$ 10%	$8490 \times 10^{-6}$ 214%	$4310 \times 10^{-6}$ 60%	$2920 \times 10^{-6}$ 8%
TIME TO MAXIMUM STRAIN (SEC) & DIFFERENCE	$3.0 \times 10^{-3}$	N/A	$2.6 \times 10^{-3}$ -13%	$3.6 \times 10^{-3}$ 19%	$2.6 \times 10^{-3}$ -12%	$3.3 \times 10^{-3}$ 10%
TIME TO ZERO STRAIN (SEC) & DIFFERENCE	$10.5 \times 10^{-3}$	N/A	$3.5 \times 10^{-3}$ -67%	$5.3 \times 10^{-3}$ -49%	$5.8 \times 10^{-3}$ -45%	$6.2 \times 10^{-3}$ -41%

Notes:

- Transient 1: Includes nonlinear loads
- Transient 2: Includes nonlinear loads and damping = 0.5/1719.592
- Transient 3: Includes nonlinear loads and damping = 0.75/1719.592

TABLE B-8. MEMBRANE-ROD FINITE ELEMENT (QDMEM2, ROD) MODEL  
VS TEST 2 FOR GAGE ET2

ANALYSIS TYPE	Experimental Test	Static	Transient	Transient 1	Transient 2	Transient 3
MAXIMUM STRAIN & DIFFERENCE	$-2250 \times 10^{-6}$	$-5500 \times 10^{-6}$ 144%	$-4820 \times 10^{-6}$ 114%	$-12300 \times 10^{-5}$ 446%	$-6690 \times 10^{-6}$ 197%	$-5440 \times 10^{-6}$ 142%
TIME TO MAXIMUM STRAIN (SEC) & DIFFERENCE	$2 \times 10^{-3}$	N/A	$2.1 \times 10^{-3}$ 5%	$3.7 \times 10^{-3}$ 83%	$2.6 \times 10^{-3}$ 29%	$2.5 \times 10^{-3}$ 25%
TIME TO ZERO STRAIN (SEC) & DIFFERENCE	$9 \times 10^{-3}$	N/A	$3.2 \times 10^{-3}$ -64%	$5.3 \times 10^{-3}$ -41%	$5.7 \times 10^{-3}$ -37%	$6.1 \times 10^{-3}$ -32%

Notes:

- Transient 1: Includes nonlinear loads
- Transient 2: Includes nonlinear loads and damping coefficient = 0.5/1719.592
- Transient 3: Includes nonlinear loads and damping coefficient = 0.75/1719.592

TABLE B-9. MEMBRANE-BENDING FINITE ELEMENT (QUAD1) MODEL  
VS TEST 1 RESULTS FOR GAGE ET4

ANALYSIS TYPE	Experimental Test	Static	Transient	Transient 1
MAXIMUM STRAIN % DIFFERENCE	$1750 \times 10^{-6}$	$3070 \times 10^{-6}$ 75%	$2530 \times 10^{-6}$ 44%	$4040 \times 10^{-6}$ 131%
TIME TO MAXIMUM STRAIN (SEC) % DIFFERENCE	$2.5 \times 10^{-3}$	N/A	$3.1 \times 10^{-3}$ 26%	$3.9 \times 10^{-3}$ 56%
TIME TO ZERO STRAIN (SEC) % DIFFERENCE	$8.5 \times 10^{-3}$	N/A	$4.3 \times 10^{-3}$ -49%	$5.7 \times 10^{-3}$ -33%

Notes:  
Transient 1: Includes nonlinear loads

TABLE B-10. MEMBRANE-BENDING FINITE ELEMENT (QUAD1) MODEL  
VS TEST 1 RESULTS FOR GAGE ETS

ANALYSIS TYPE	Experimental Test	Static	Transient	Transient 1
MAXIMUM STRAIN & DIFFERENCE	$-2100 \times 10^{-6}$	$-5060 \times 10^{-6}$ 141%	$-3970 \times 10^{-6}$ 89%	$-6760 \times 10^{-6}$ 222%
TIME TO MAXIMUM STRAIN (SEC) & DIFFERENCE	$2.5 \times 10^{-3}$	N/A	$3.3 \times 10^{-3}$ 30%	$4.0 \times 10^{-3}$ 58%
TIME TO ZERO STRAIN (SEC) & DIFFERENCE	$10 \times 10^{-3}$	N/A	$4.5 \times 10^{-3}$ -55%	$6.0 \times 10^{-3}$ -40%

Notes:  
Transient 1: Includes nonlinear loads

TABLE B-11. MEMBRANE-BENDING AND ROD FINITE ELEMENT (QUAD1, BAR)  
MODEL VS TEST 1 RESULTS FOR GAGE ET4

ANALYSIS TYPE	Experimental Test	Static	Transient	Transient 1
MAXIMUM STRAIN & DIFFERENCE	$1750 \times 10^{-6}$	$520 \times 10^{-6}$ -70%	$370 \times 10^{-6}$ -79%	$690 \times 10^{-6}$ -61%
TIME TO MAXIMUM STRAIN (SEC) & DIFFERENCE	$2.5 \times 10^{-3}$	N/A	$2.8 \times 10^{-3}$ 14%	$3.7 \times 10^{-3}$ 46%
TIME TO ZERO STRAIN (SEC) & DIFFERENCE	$8.5 \times 10^{-3}$	N/A	$4.1 \times 10^{-3}$ -52%	$5.3 \times 10^{-3}$ -37%

Notes:  
Transient 1: Includes nonlinear loads

TABLE B-12. MEMBRANE-BENDING AND ROD FINITE ELEMENT (QUAD1, BAR)  
MODEL VS TEST 1 RESULTS FOR GAGE ET5

ANALYSIS TYPE	Experimental Test	Static	Transient	Transient 1
MAXIMUM STRAIN & DIFFERENCE	$-2100 \times 10^{-6}$	$-1780 \times 10^{-6}$ -15%	$-1690 \times 10^{-6}$ -19%	$-2690 \times 10^{-6}$ 28%
TIME TO MAXIMUM STRAIN (SEC) & DIFFERENCE	$2.5 \times 10^{-3}$	N/A	$2.7 \times 10^{-3}$ 10%	$3.4 \times 10^{-3}$ 37%
TIME TO ZERO STRAIN (SEC) & DIFFERENCE	$10 \times 10^{-3}$	N/A	$3.9 \times 10^{-3}$ -61%	$5.2 \times 10^{-3}$ -48%

Notes:  
Transient 1: Includes nonlinear loads



TABLE B-13. MATERIAL AND SECTION PROPERTIES FOR QUARTER-SCALE MODEL

Concrete

$$E = 4.25 \times 10^6 \text{ psi}$$

$$G = 1.77 \times 10^6 \text{ psi}$$

$$\text{Poisson's Ratio} = 0.2$$

$$\text{Unit Weight} = 150 \text{ pcf}$$

$$\text{Unit Mass} = 0.000216 \text{ lb sec}^2/\text{in}^4$$

Steel

$$E = 29.0 \times 10^6 \text{ psi}$$

$$G = 11.2 \times 10^6 \text{ psi}$$

$$\text{Poisson's Ratio} = 0.3$$

$$\text{Unit Mass} = 0.000735 \text{ lb sec}^2/\text{in}^4$$

Soil

$$\text{Unit Weight} = 110 \text{ pcf}$$

Structural Element	Clear Span (in)	Thickness (in)	Flexural Depth (in)	Steel Area (in <sup>2</sup> )
Roof	48	9	8	1.32 each face
Exterior Wall	48	9	8	1.32 each face
Interior Wall	48	6	*5	*0.66 each face
Floor	48	6	*5	*0.82 each face

\* Assumed Values

## APPENDIX C

### DISPLACEMENT APPROACH RIGID FORMATS

#### INTRODUCTION

The NASTRAN (NASA Structural Analysis) Computer Program is a general-purpose structural analysis program intended for a wide range of applications. To meet this requirement NASTRAN contains different finite elements to represent common construction members and allows these elements to be combined to model more sophisticated construction materials. NASTRAN currently provides 15 different methods to determine displacements of a structure. Each method is referred to as a Displacement Approach Rigid Format and the user chooses the rigid format, depending on the type of analysis required (Reference 15).

To improve the generality of NASTRAN the program is divided into subprograms or modules that can be called independently of each other. A rigid format is a permanently stored sequence of subprogram calls which produce a particular kind of structural analysis. The user may alter the sequence of calls or develop a new sequence for unusual analysis problems (Reference 13).

One of the subprograms available for use with any rigid format is the Plot Module. The plotting routines allow plotting of specific input and output data on a SC-4020 plotter, an Electronic Association Incorporated plotter, and most Calcomp plotters. Also a user may write his own plotter routines for use with NASTRAN (Reference 13).

Some rigid formats yield large amounts of numerical output. Output in graphical form gives the engineer a better feeling for the response of the structure. Figures A-1, A-2, A-3, A-4, A-5, and A-6 are samples of the type of output available through the NASTRAN Plot Module. Undeformed structural plots aid in the detection of input errors in grid point coordinates and element connections.

For this investigation two rigid formats were used, Static and Transient. Two other rigid formats, Piecewise Linear and Differential Stiffness may be useful. The remainder of this appendix is a brief discussion of those rigid formats, emphasizing the portions of those formats that are useful in analyzing hardened structures.

#### STATIC DISPLACEMENT APPROACH RIGID FORMAT

The Static Analysis Rigid Format is used to determine deformation, stresses, etc, caused by very slowly applied loads. This rigid format is a good starting point in any analysis because the designer can check for input errors in the finite element model and for conceptual errors in the choice of elements and boundary conditions.

The loads may be concentrated at grid points, uniformly distributed over two-dimensional finite elements, and generated internally as body forces caused by gravity. NASTRAN will compute the gravity loads from the mass matrix if the gravity acceleration vector is input. The mass matrix is composed of the element mass and any nonstructural mass applied to the element, for example, soil above an underground structure (Reference 12). Different load factors may be applied to each load to aid in "limit state" design.

Solving the set of simultaneous equations generated by the finite element method uses large amounts of computer resources. The Static Analysis Rigid Format is set up to analyze the structure for different loading combinations and/or different boundary conditions without resolving the set of simultaneous equations. Each loading combination and each new set of boundary conditions is called a subcase.

#### TRANSIENT APPROACH RIGID FORMAT

To solve structural dynamic problems the Transient Approach Rigid Format is used. This approach assembles the structural stiffness, mass, and damping matrices; generates time history load tables; and solves the differential equations by a form of the Newmark Beta Method. The stiffness, mass, and damping matrices may be assembled by NASTRAN and/or directly input by the user (Reference 12).

Because of the large number of load entries required for even a moderate size problem, NASTRAN provides four different functions, three linear functions and one power function, to input dynamic loads. In addition to those loads NASTRAN can generate nonlinear loads triggered by the deflections and/or velocities of grid points (Reference 12). Nonlinear loads provide a means of modeling nonlinear material behavior.

Mass matrices are generated by either the Lumped Mass or Coupled Mass Methods. Some individual elements have restrictions on the method of mass matrix generation allowed. Also, masses may be assigned directly to grid points (Reference 12).

The Lumped Mass Method distributes the structural mass and nonstructural mass evenly between the nodes of the element. This yields a simpler model because there is no inertia coupling between grid points. In most cases the Lumped Mass Method will result in natural frequencies below the true value (Reference 12).

The Coupled Mass Method, sometimes called "Consistent" Mass Method, yields an inertia coupling between grid points, i.e., the inertia properties of a grid point affect the inertia properties of adjacent grid points. The element mass matrix is dependent on the elastic properties of the element. This method normally yields natural frequencies above the exact results (Reference 12).

The damping matrix is the sum of direct input damping coefficients from viscous damping elements, a percentage of the structure stiffness matrix, and a percentage of any/all element stiffness matrices. The user specifies the appropriate constants for NASTRAN to compute the damping matrix. If the input data is not specified, structural damping is neglected. Normally structural damping is expressed as a percentage of the critical damping (Reference 2). NASTRAN does not contain a convenient way of expressing damping in this manner.

For this rigid format graphical output is particularly useful. Plots of element stresses and forces versus time, and grid point deflections and velocities versus time are available. Also deformed and undeformed structure plots are available in three dimensions.

#### PIECEWISE LINEAR APPROACH RIGID FORMAT

Piecewise Linear Analysis is used to solve problems involving material plasticity. This rigid format is presently restricted to statically applied loads. Since the loads cannot be varied with time, it is not applicable to the analysis of hardened structures in its present form and was not included in this investigation.

For the Piecewise Linear Approach the user specifies a material stress-strain table and the amount of load to be applied in each increment. The rigid format proceeds to determine the displacements and strain using the first load increment and the user-specified elastic material properties (not the user provided stress-strain table). NASTRAN then uses extrapolation to determine the strain expected in the next load increment. With this projected strain a linear approximation for the modulus of elasticity for each element is calculated from the stress-strain table. A new stiffness matrix is assembled and the deflections and strains for the next load increment are determined. Deflections and strains are accumulated after each load increment. The rigid format repeats the sequence beginning with the extrapolation to estimate the next strain and continues until the total load has been applied (Reference 12). Solving the simultaneous equations for each load increment requires huge amounts of computer resources. Choosing too many steps uses an unnecessary amount of computer resources; however, too few steps will make the solution inaccurate.

Piecewise Linear Analysis also generates large amounts of output data. The plotting capabilities of the plot modules provide output in a more useful form.

#### DIFFERENTIAL STIFFNESS APPROACH RIGID FORMAT

In some structural problems deformations occur that adversely affect the structures' ability to carry the loads. In the design of tall steel buildings this is referred to as the P-Delta effect.

This rigid format introduces nonlinearity into the analysis caused by large deflections. The NASTRAN approach is an approximate analysis and may not be applicable to a particular problem, so that the use of this rigid format must be carefully reviewed. One important limitation is that applied loads remain fixed in direction and magnitude during the movement of the structure (Reference 12).

In some hardened structures this rigid format may prove useful; however, when reinforced concrete is the construction material failure of the concrete will occur before the deflections affect the structural capacity (Reference 16). The Differential Stiffness Approach Rigid Format was not investigated in this report.

## APPENDIX D

### NASTRAN FINITE ELEMENTS

#### INTRODUCTION

Only a few of the available finite elements were used in this investigation. This appendix lists those elements and contains a brief description of the important element properties.

The NASTRAN plate membrane elements were developed by constructing the expression for strain energy using a linear variation in the inplane displacements. The basic element is triangular (TRMEM) and is used to form other quadrilateral elements. The quadrilateral elements are formed by either overlapping four triangular elements (QDMEM) or by connecting four triangular elements (QDMEM2) at the center point of the quadrilateral (Reference 12).

The material properties for the elements may be anisotropic; however, only isotropic material was used in this investigation (Reference 14). For an isotropic material two of three material constants, modulus of elasticity, shear modulus, or Poisson's ratio must be specified.

The Lumped Mass Method for transferring structural and nonstructural mass to adjacent grid points is the only method available for membrane elements. The mass matrix and inplane stiffness for the elements are found by assigning one half the thickness of the quadrilateral element to each triangular element. Although the Coupled Mass Method cannot be used for structural models with membrane stiffness only, the method may be specified for elements with both bending and membrane stiffness. The terms in the mass matrix which correspond to inplane motions are computed by the Lumped Mass Method and the other mass terms will be computed by the Coupled Mass Method (Reference 12).

The strains within this element are constant because the deflections were assumed to be linear, so the stresses are an average within each element. The state of stress for a nonoverlapping element is the average stress in the four triangular elements. A "shear flow" is calculated for the sides of each element. The "shear flow" is the change in the inplane force along the side divided by the length of the side (Reference 12).

#### ROD ELEMENT

The rod element (ROD) developed for NASTRAN includes extensional and torsional properties only and is based on a linear deformation function. The elements are straight, loaded at the ends only, and have uniform geometric and material properties. The strains are constant for the element because of the linear deformation functions and the stresses are on average for the element (Reference 12).

For dynamic analysis approaches the structural and nonstructural mass associated with each rod may be transferred to the adjacent grid points by the Lumped Mass or Coupled Mass Methods. For this element the coupled mass matrix is the average of the pure lumped mass and the pure coupled mass matrices. This yields a much smaller error in the natural frequency than either the Lumped Mass or Coupled Mass Methods alone (Reference 12).

#### PLATE BENDING ELEMENT

The basic NASTRAN plate-bending element (TRPLT) is a triangle with three degrees of freedom, one translational and two rotational, at each node. The out-of-plane deflection is assumed to be the following incomplete third-degree function (Reference 12).

$$w = ax + by + cx^2 + dxy + ey^2 + fx^3 + gxy^2 + hy^3$$

The  $x^2y$  term is omitted because there are only eight independent deformations in the triangular element, and only eight constants can be determined in the out-of-plane deflection field. This displacement does not guarantee slope continuity on the edges of adjacent elements; however, elements which have slope continuity do not necessarily give better results (Reference 8).

The plate-bending element may be an anisotropic material and the user can specify material properties with respect to any axis orientation. The program will rotate the properties into the proper coordinate system. As with the plate-membrane element, two of the three material constants must be specified (Reference 13).

The element may be assumed rigid in transverse shear. This decreases the magnitude of the element stiffness terms by an amount equal to the transverse shear stiffness (Reference 12). In beam elements transverse shear stiffness is normally omitted because of its small size. In hardened structures transverse shear stiffness is important because of the thickness of the construction and should not be neglected.

The internal forces are determined at the center of gravity of the triangular element. A linear variation of strain through the thickness of the plate is assumed, so stresses may be determined at any distance from the middle surface (Reference 12).

The Lumped Mass and Coupled Mass Methods are available to create mass matrices for plate bending elements. The Lumped Mass Method places one third of the element mass at each node. In the Coupled Mass Method, the mass matrix of each element is calculated assuming a uniform mass density within the element. Thus the mass matrix depends on the bending properties of the plate element (Reference 12).

A quadrilateral plate-bending element (QDPLT) is formed by overlapping four triangular bending elements. The bending stiffness of each triangular element is one half the bending stiffness of the quadrilateral element. The mass matrix is formed by treating the quadrilateral as four triangular elements. The stresses are the average of the stresses in each triangular element (Reference 12).

#### PLATE-BENDING-MEMBRANE ELEMENT

Small deflection theory for plates leads to independence between membrane (inplane) forces and bending (out-of-plane) forces (Reference 11). NASTRAN forms a plate-bending-membrane element by overlapping the quadrilateral membrane element, QDMEM (composed of four overlapping triangular elements), and the bending quadrilateral, QDPLT (composed of four overlapping elements). Two plate-bending-membrane elements are formed; QUAD1 in which the different material properties may be specified for bending, membrane and transverse shear, and QUAD2 which assumes a solid homogeneous cross section (Reference 13).

The mass matrices may be formed by using the Lumped Mass or Coupled Mass Method for the bending stiffness. The Lumped Mass Method will be used for the membrane stiffness (Reference 12).

Element stresses are available at any location away from the middle surface. Also bending stresses of the plate combined with the membrane stresses are available.

#### Beam Elements

The beam element (BAR) is derived, assuming a straight beam loaded only at the ends and having uniform geometric and material properties along its length. The directions of the principal axis may be selected by the user and the ends of the beam element may be offset from the grid point to which the beam is attached. The connection between the beam end and the corresponding grid point may be released for any degree of freedom provided one degree of freedom remains (Reference 12).

The stiffness matrix includes extensional, torsional, and bending in two planes. The bending stiffness also includes a contribution due to transverse shear (Reference 12).

Internal forces and moments are computed on the ends of the element. Stresses at each end due to bending at user's specified points may be determined along with the average axial stress and the maximum and minimum extensional stresses (Reference 12).

Lumped Mass and Coupled Mass Methods are available to transfer structural and nonstructural mass to the adjacent grid points. The center of gravity is assumed to lie on the elastic axis and the inertia effects due to offset ends of beams are neglected. The Coupled Mass Method does not include the effect of transverse shear on the mass matrix (Reference 12).



## APPENDIX E

### QUARTER-SCALE UNDERGROUND SHELTER TEST

The data used to judge the finite element models came from a one-quarter scale model test of an underground shelter (see Reference 4). The tests were conducted to verify procedures for predicting shelter response and shelter loading caused by an explosion on a covering burster slab (see Figure E-1). All 14 test were run and a large amount of data was collected. For this investigation only the interface stresses from pressure gages on the top of the roof and the strain in the reinforcing steel from Test 1 and Test 2 were used. A more detailed report on the test is being prepared and only preliminary data was available for this analysis.

Generally the pressure gages functioned well for both tests and provided the loads for the finite element model. A typical pressure time curve is shown in Figure E-2. The gage at the face of the exterior wall failed in Test 1 and the pressure from the gage at the face of the interior wall was substituted (see Figure E-1).

The strain gage data was spotty because many gages failed under the high strain rates. Good strain data were available from Tests 1 and 2 at the centerline of the roof span and at the face of the interior wall (see Figures E-1 and E-3). Since one gage was in a tension zone and the other was in a compression zone, these two points were chosen to judge the accuracy of the computer models.

Table B-13 contains the properties used in the finite element models. The section property data were incomplete and assumed values were used. The missing information was for the walls and floor so they should not be critical to the structural analysis.

The quarter scale test contained a weighted average for the interfaced pressure gages for each explosion. No information was given concerning how the weighted average was computed (Reference 4). This value was used for the Static Analysis Approaches.

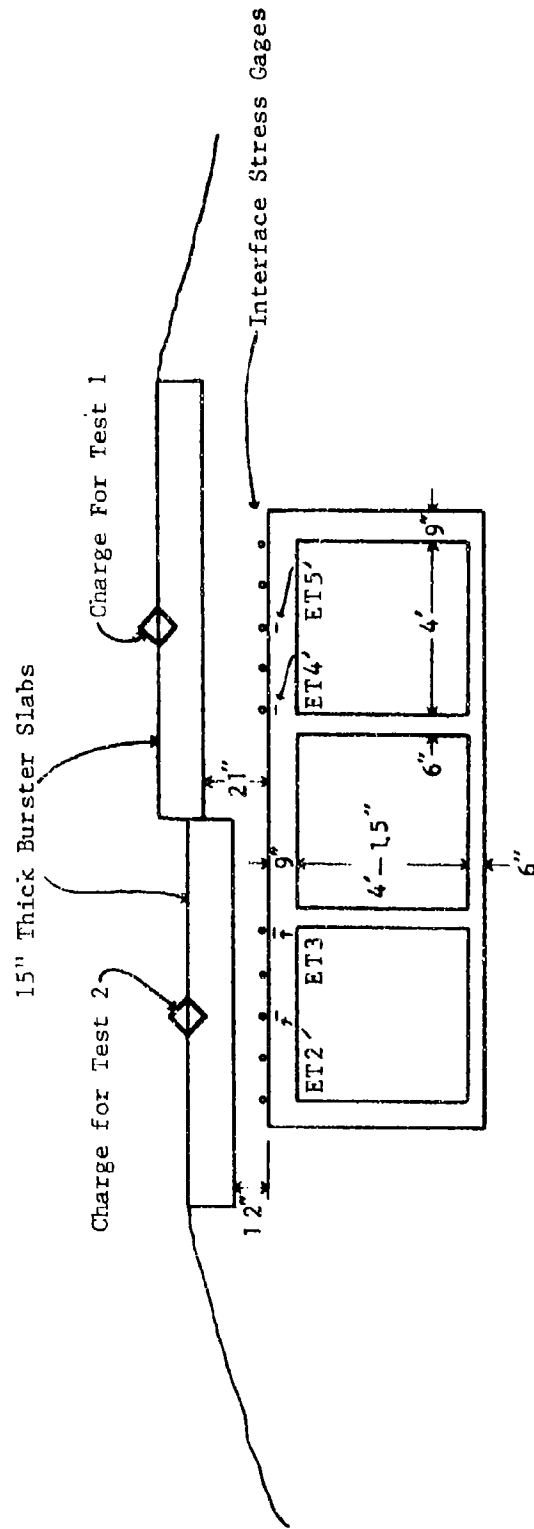


FIGURE E-1. Charge and Gage Locations for Test Shelter

200000. HZ CGL= 3809.

✱ ✱

14291- 70 09/12/90 R0955

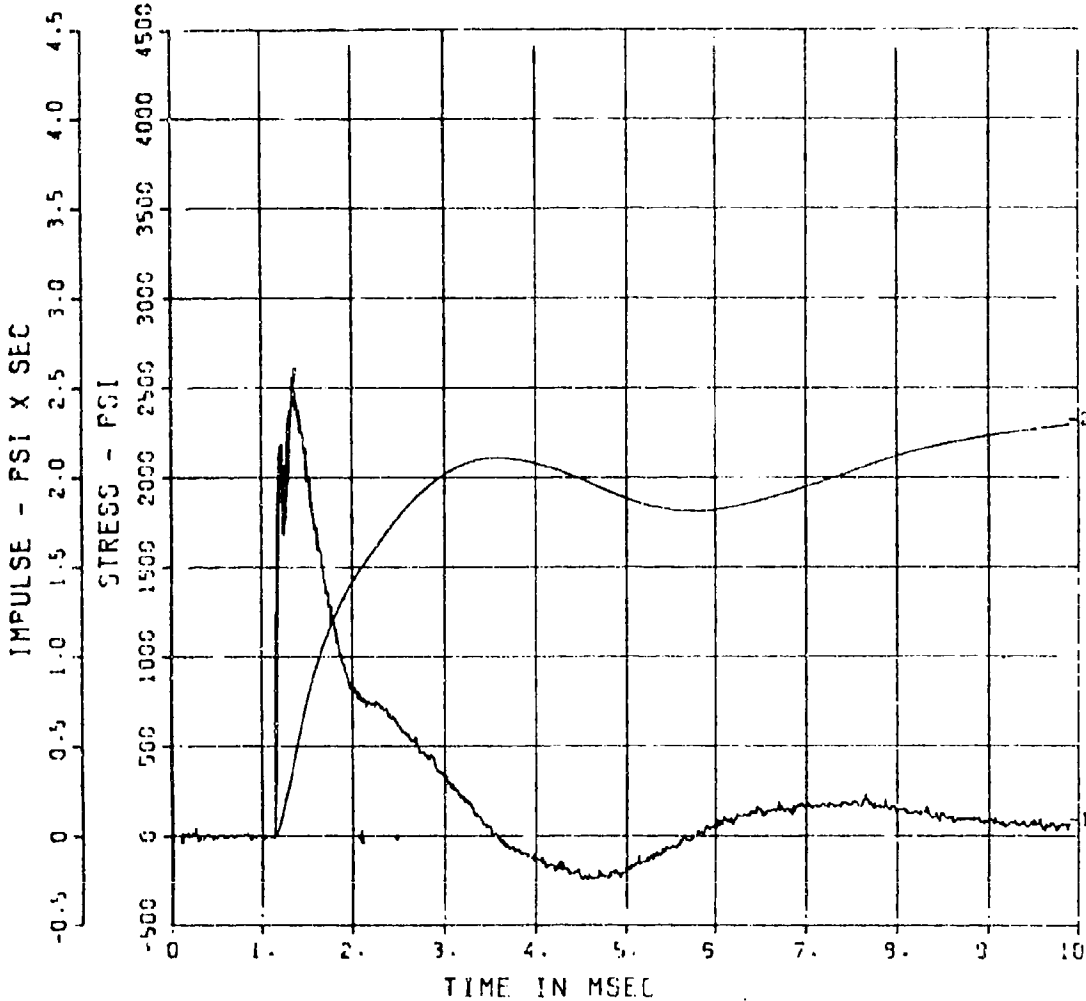


FIGURE E-2. Typical Pressure-Time Curve From Shelter Test

SHELTER TEST 1  
LT4  
200000. HZ CAL= 2337.  
LP4 70% CUTOFF= 3000. HZ

\*\*

\*\*

14201- 5 11/13/90 R0305

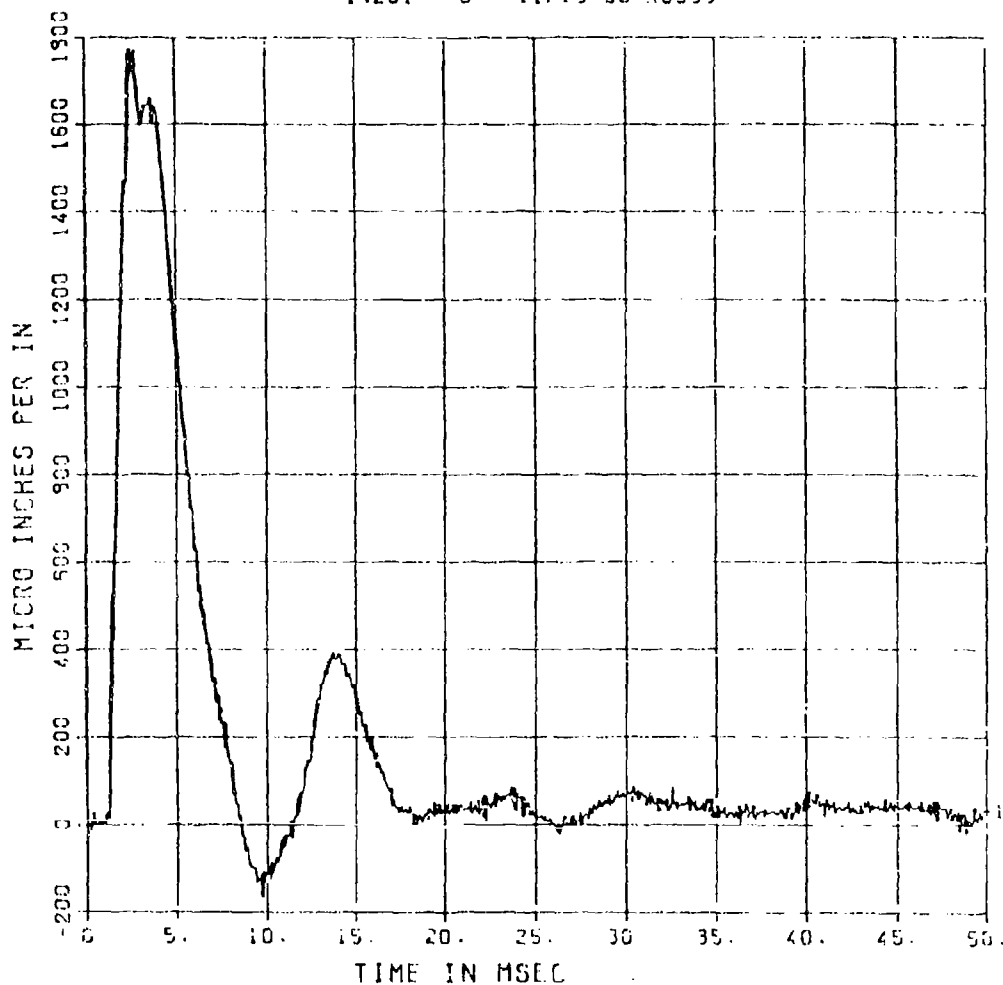


FIGURE E-3. Typical Strain-Time Curve From Shelter Test

## APPENDIX F

### RESISTANCE-DEFLECTION FUNCTIONS

In response to externally applied loads a structural member deflects a sufficient amount to develop enough internal force to preserve equilibrium. These internal forces can be considered as an equivalent load. Resistance is in the direction opposite the deflection. Since this equivalent load and the deflections are based on geometric and material properties, a graphical representation of resistance versus deflection can be drawn independently of the applied external loads (Reference 10).

For a reinforced concrete member the initial response is elastic and the elastic response continues until the deflection is sufficient to cause first cracking in the tension zone. However, the nonlinearity induced by the initial cracks is negligible and a linear resistance deformation function may be used until first yield in the reinforcing steel. After first yield in the reinforcing steel the response of a reinforced concrete member is termed elasto-plastic and sufficient cracking has occurred to require a reduced stiffness in order to model the response in the reinforced concrete member. The upper limit of the elasto-plastic region is the formation of the first plastic hinge. From this point the member's resistance will remain constant until incipient failure of the member occurs (Reference 10).

The resistance deflection functions were calculated as described in Reference 10, except for the ultimate resistance of the reinforced concrete member. The equations given in Reference 10 to calculate the ultimate moment resistance of a reinforced concrete member neglect the contribution due to the compression concrete area. This would underestimate the strength of the concrete member in the elasto-plastic range. After enough rotation to cause crushing of the compression concrete area the equation given will accurately predict the ultimate capacity. The following equation was used to predict the ultimate capacity of the shelter (Reference 16).

$$M_n = A_s f_y (d - a/2) - A'_s f'_s (d' - a/2)$$

in which

$A_s$  = tension steel area

$f_y$  = tension steel yield stress

$d$  = distance from compression face to centroid of tension steel

$d'$  = distance from compression face to centroid of compression steel

$A'_s$  = compression steel area

$f'_s$  = stress in compression steel

$a$  = depth of Whitney's stress block

$M_n$  = ultimate (nominal) moment